

Source Terms, Shielding Calculations and Soil Activation for a Medical Cyclotron

Konheiser, J.; Naumann, B.; Ferrari, A.; Brachem, C.; Müller, S.;

Originally published:

October 2016

Journal of Radiological Protection 36(2016), 819

DOI: <https://doi.org/10.1088/0952-4746/36/4/819>

Perma-Link to Publication Repository of HZDR:

<https://www.hzdr.de/publications/Publ-21269>

Release of the secondary publication
on the basis of the German Copyright Law § 38 Section 4.

Source terms, shielding calculations and soil activation for a medical cyclotron

J Konheiser^{1,*}, B Naumann¹, A Ferrari¹, C Brachem², S E Müller¹

¹Helmholtz-Zentrum Dresden-Rossendorf, Postfach 510119, 01314 Dresden, Germany

²Technische Universität Dresden, 01062 Dresden, Germany

*Corresponding author: j.konheiser@hzdr.de

Abstract

Calculations of the shielding and estimates of soil activation for a medical cyclotron are presented in this work. Based on the neutron source term from the $^{18}\text{O}(p,n)^{18}\text{F}$ reaction produced by a 28 MeV proton beam, neutron and gamma dose rates outside the building were estimated with the Monte Carlo code MCNP6 (Goorley *et al* 2012 *Nucl. Technol.* **180** 298–315). The neutron source term was calculated with the MCNP6 code and FLUKA (Ferrari *et al* 2005 INFN/TC_05/11, SLAC-R-773) code as well as with supplied data by the manufacturer. MCNP and FLUKA calculations yielded comparable results, while the neutron yield obtained using the manufacturer-supplied information is about a factor of 5 smaller. The difference is attributed to the missing channels in the manufacturer-supplied neutron source terms which considers only the $^{18}\text{O}(p,n)^{18}\text{F}$ reaction, whereas the MCNP and FLUKA calculations include additional neutron reaction channels. Soil activation was performed using the FLUKA code.

The estimated dose rate based on MCNP6 calculations in the public area is about 0.035 $\mu\text{Sv/h}$ and thus significantly below the reference value of 0.5 $\mu\text{Sv/h}$ (2011 *Strahlenschutzverordnung*, 9 Auflage vom 01.11.2011, Bundesanzeiger Verlag). After 5 years of continuous beam operation and a subsequent decay time of 30 days, the activity concentration of the soil is about 0.34 Bq/g.

Keywords: neutron source terms, shielding calculation, soil activation, cyclotron

1. Introduction

In recent years the need for cyclotron-produced radionuclides for positron emission tomography (PET) and for other medical applications has strongly increased. The majority of these radionuclides are produced by proton bombardment of selected targets at dedicated cyclotrons. Neutrons and photons produced in the induced nuclear reactions are the main source of radioactive dose rate outside of the building and drive the shielding design. The neutron radiation imposes particularly high requirements for radiation protection, because neutrons, being uncharged, are deeply penetrating, and they can produce highly ionizing secondary radiation. Many publications [4, 5, 6, 7 and 8] exist for shielding calculations of neutrons produced in radionuclide production. In these publications, building structures are different and proton energies are usually lower and therefore do not meet our requirements.

In the framework of the recently established "Center of Radiopharmaceutical Cancer Research" a TR-FLEX cyclotron from the company "ADVANCED CYCLOTRON SYSTEMS INC." (ACSI, Richmond, BC, Canada) will be installed in the Helmholtz-Zentrum Dresden-Rossendorf (HZDR). It will be located in a basement which is partially above ground level, with a public road passing close to the building. The cyclotron basement bunker is built from reinforced concrete (density 2.35 g/cm³), with a wall thickness of 270 cm. The thickness of the ground plate is 60 cm. The proton energy of the cyclotron TR-FLEX at HZDR will be up to 28 MeV with a maximum current of 300 μA . It must be guaranteed that under these conditions, the reference dose rate limit of 0.5 $\mu\text{Sv/h}$ outside the cyclotron bunker is not exceeded.

In a first phase of the design for the "Center of Radiopharmaceutical Cancer Research" the installation of a TR-24 cyclotron with maximum proton energy of 24 MeV was foreseen. With the release of the TR-FLEX it was decided to increase the proton energy to 28 MeV, and it was therefore investigated whether the radiation protection is guaranteed with the higher proton energy. Additional calculations were done concerning the soil activation below the ground plate by the neutron radiation.

Figure 1 shows a vertical section view of the cyclotron bunker including several key points for radiation protection. The water target (point T) is located about 100 cm from the building wall at beam height (150 cm). Dose rates were calculated for all points at maximum beam power. The distance of all points from the outer

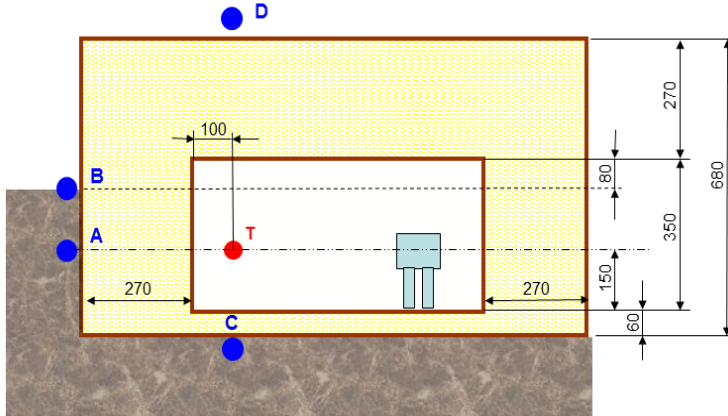


Figure 1: Vertical schematic view of the cyclotron room, indicating the position of the target (T) and the key points for the calculations (A,B,C,D). All dimensions are in cm.

surface of the wall is 20 cm. Point A is located at beam height, point B is located 20 cm above the road level and point D, positioned vertically above the target, is the most exposed point above the ceiling. The activation of the soil is estimated at point C, which is positioned vertically below the target, just below the ground plate.

The shielding calculations were carried out on the basis of radiation that is formed during the production of the radioactive nuclide ^{18}F , obtained by proton bombardment of a ^{18}O -enriched water target via the $^{18}\text{O}(p,n)^{18}\text{F}$ reaction. ^{18}F is used for marking fluorodeoxyglucose (FDG) [9], one of the most commonly used radio-pharmaceuticals. With a proton beam current of $300\ \mu\text{A}$, the production of ^{18}F generates the largest amount of neutron radiation compared to other processes. Because neutron radiation is the most important issue to be considered in shielding calculations, the presented results are based on neutron emission in the $^{18}\text{O}(p,n)^{18}\text{F}$ reaction.

The neutron source terms were either provided by the manufacturer, or calculated using MCNP6 and FLUKA Monte Carlo programs (see detailed discussion below). In order to increase the efficiency of the calculations, a two-step process was used in which pre-calculated source term distributions were supplied to the actual shielding calculations. These were performed using the MCNP6 program. Fluence Φ to ambient dose equivalent $H^*(10)$ conversion coefficients $H^*(10)/\Phi$ -ICRU57 [10] for neutrons and photons were used to calculate dose rates from particle fluence rates. These conversion coefficients are the conversion factors of the ICRP Publication 74 [11].

2. The model for the shielding calculation and the material parameters

Figures 2 and 3 show schematic views of the geometry model used in the MCNP6 simulation. It is common practice in Monte Carlo simulations to only model the regions relevant to the result. Therefore, to optimize the calculation of the dose rate outside the building, only the wall with the outer surface towards the street was modeled with the corresponding thickness of 270 cm. All other walls were modeled only with a thickness of 25 cm, to take into account the scattered neutron radiation from the walls, since pre-calculations show that the tenth value thickness of concrete is approximately 25 cm. The part of the omitted neutrons is therefore on the order of 1%. The effect on the results is in reality even smaller because the omitted neutrons have their energy reduced from flying through the concrete. Therefore, the impact of the reduced wall thickness on the results can be considered insignificant. For the calculation of the fluences below the ground plate (point C) and above ceiling (point D) separate calculations with the real thicknesses (60 cm and 270 cm) were done. Because the neutron and gamma fluence rates decrease by several orders of magnitude along the wall thickness, the use of variance reducing techniques is essential. Geometry splitting/Russian roulette is one of the oldest, most widely used and effective techniques in Monte Carlo simulations. For these reasons, the 270 cm wall was divided into 14 equally thick layers to allow for the introduction of zone weights. Correspondingly, the 60 cm ground plate was divided into 3 layers. This division is again based on the tenth value thickness.

The cyclotron was modeled as a rectangular block of pure iron to simulate possible scattering of neutrons by the cyclotron. The block has the external dimensions of the cyclotron, and was placed at the cyclotron's position. All other installations have been neglected. Since local specifications are not available, the material composition of the concrete was taken from ref. 12. Table 1 shows the elemental composition of the concrete. The concrete density

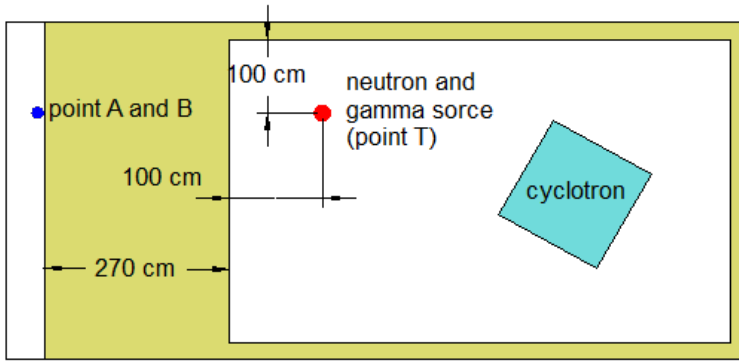


Figure 2: Horizontal schematic view the MCNP calculation model for point A and B.

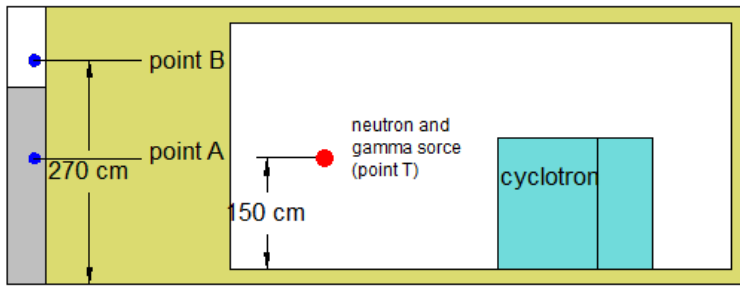


Figure 3: Vertical schematic view the MCNP calculation model for point A and B.

was 2.35 g/cm³. The reinforcing steel in the concrete was not simulated. It can therefore be assumed that the results are overestimated due to the absence of neutron and gamma absorption by steel. The calculations with MCNP6 were performed using the included standard data libraries based on the evaluated nuclear data file ENDF/B-VII.1 [13].

Table 1: Element mix of the concrete from ref. 12:

Element	Weight percent	Element	Weight percent
O	51.02 %	Al	1.43 %
Ca	25.05 %	Fe	0.92 %
Si	14.83 %	H	0.82 %
C	5.83 %	S	0.10 %

3. The neutron source term

Three ways to evaluate the neutron source term were followed in this work:

- a manufacturer-supplied normalized neutron spectrum together with a scale factor for the total neutron yield [14] was taken,
- a source term calculation using the recently released MCNP6 code was used and
- the source term was calculated using the FLUKA code.

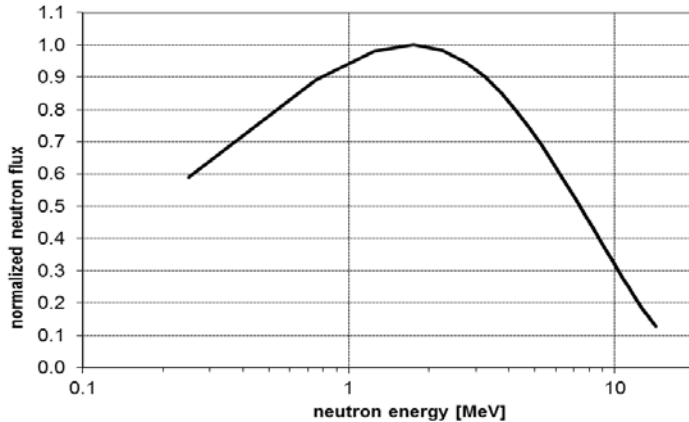


Figure 4: Normalized spectrum to the maximum value of source neutrons as function of the energy provided by the manufacturer.

The first neutron spectrum in the list above was extracted from a report provided by the manufacturer of the cyclotron. It was calculated with the program ALICE-91 [15], assuming a proton beam energy of 24 MeV. The ALICE-91 code calculates nuclear reaction on the basis of the Weisskopf-Ewing evaporation model [16]. Since the calculations were carried out by the manufacturer of the cyclotron, not much information is available about the calculations itself. Figure 4 shows the normalized spectrum of source neutrons as function of the energy provided by ref. 14. The total number of emitted neutrons per 1 $\mu\text{A}\cdot\text{h}$ primary protons for the $^{18}\text{O}(p,n)^{18}\text{F}$ reaction is reported to be $3.8\cdot 10^{13}$. For an assumed proton current of 300 μA the neutron source strength is $3.17\cdot 10^{12}$ neutrons/s.

With the MCNP6 code it is possible to calculate the neutron source term directly and therefore this code was used to crosscheck the manufacturer-supplied data. The calculation model for the source term evaluation consists of a cylinder with a radius of 0.55 cm and a length of 4 cm. The volume is filled with water enriched with 97 % ^{18}O . The volume is enclosed with a 0.1 mm thick niobium mantle. The dimensions correspond to the ones of the actual irradiation target. The emitted neutron spectrum is determined on the surface of a surrounding sphere. The radius of the sphere is 10 m, large enough to minimize geometrical effects due to the target shape. In addition, the sphere is divided into four equal areas in order to determine possible directional dependencies.

Evaluated nuclear data were used by MCNP6 for the characterization of the (p,n) reaction. The calculation of the reaction was carried out with the nuclear data library TENDL, an evaluated data file based on the nuclear model code TALYS [17]. Since ^{18}O -data are not included in the standard library of MCNP6, they were generated using the NJOY [18] program and imported into MCNP6. Two models were assumed for the shape of the proton beam. An infinitesimal (point-like) beam was used in the first model, while a circular (surface) one was applied in the second. In the case of the surface beam a Gaussian distribution was assumed with a standard deviation of 0.125 cm, truncated at the target radius. These assumptions correspond to general beam parameters.

Table 2: Emitted neutrons per incident proton of the calculations with the different simulation codes, beam conditions and reaction data or models:

Code	E_{prot} in MeV	shape of beam	reaction data or model	neutron yield (neutrons/proton)	stat. unc.
ACSI Supplied [7]	24	-	-	0.0017	
MCNP6	24	p-like*	TENDL	0.0088	0.20 %
	24	surface		0.0087	0.20 %
	28	p-like		0.0130	0.20 %
	28	surface		0.0114	0.13 %
FLUKA	24	p-like	PEANUT	0.0104	0.04 %
	24	surface		0.0104	0.04 %
	28	p-like		0.0144	0.04 %
	28	surface		0.0145	0.04 %

*point-like

To cross-check the MCNP6 results, the neutron source terms were also determined with FLUKA. The code allows calculating the neutron source term using the pre-equilibrium cascade model PEANUT [19] for the nuclear interactions, while the interactions of neutrons with energy below 20 MeV are evaluated using data libraries ENDF/BVI.8 [20]. Since these neutron cross section libraries do not contain ^{18}O data, ^{16}O data were used instead. Geometry and beam parameters were chosen identically to the MCNP6 calculations.

Table 2 shows the number of emitted neutrons per incident proton of the calculations with the different simulation codes, beam shapes and reaction data or models, both for the nominal value of 24 MeV for the TR-24-cyclotron's proton beam as well as the value of 28 MeV for the upgraded version of the cyclotron (TR-FLEX). For the yield derived from the manufacturer-supplied information, only a value at 24 MeV is available.

The FLUKA results agree with the ones of MCNP6 between approximately 20% at 24 MeV and up to 27% at 28 MeV. The neutron yield increases from 31 % (MCNP6, surface) up to 47 % (MCNP6, point-like) if the proton energy increases from 24 MeV to 28 MeV. In all calculations the influence of the different beam shapes is smaller than 14 %. In contrast, the neutron yield obtained using the manufacturer-supplied information is about a factor of 5 smaller. This explanation is consistent with observations in ref. 21, where a significant difference for neutron yields between evaluations with tabulated yield values for the $^{18}\text{O}(p,n)^{18}\text{F}$ reaction from ref. 22 and more complex calculations was found at 17 MeV proton energies. This may be attributed to the omission of additional neutron reaction channels. For example, in ref. 17 different reaction channels are determined with neutron production. In this cross section library the (p,np) cross-section is approximately 20 times larger than the (p,n) cross-section.

Figure 5 shows the different neutron spectra for a proton current of 300 μA and energy of 24 MeV. The curves show the MCNP6 and FLUKA results with point-like and surface beam and the results obtained from the manufacturer's report (ACSI). The spectra of the MCNP6 and FLUKA calculations of the point-like source and the surface source are practically indistinguishable. This suggests that the effect of the neutron interactions in the target is negligible. The FLUKA/MCNP6 differences at 24 MeV in the neutron yield come mainly from energies below 1 MeV.

The discrepancy to the ACSI results is clearly visible. While at about 12 MeV the results of the three codes agree, at lower energies the ACSI values are up to one order of magnitude smaller respect to the MCNP6 and FLUKA calculations.

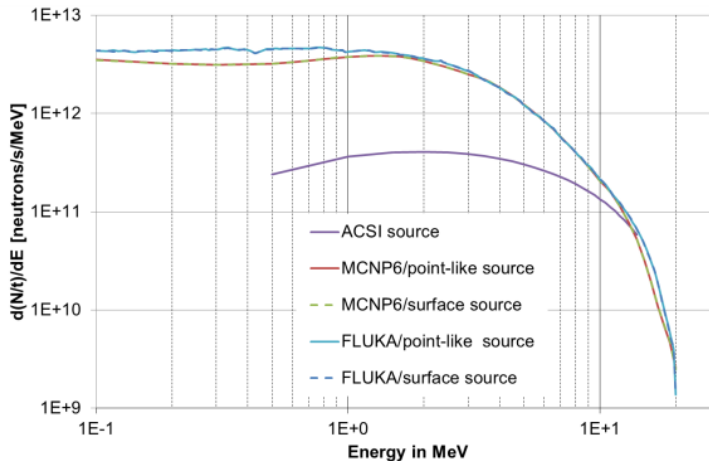


Figure 5: Spectra of neutron rate per MeV of different calculations for the proton energy of 24 MeV and a current of 300 μA .

Fig. 6 shows the differences in the neutron spectra for 24 MeV and 28 MeV from MCNP6 and FLUKA calculations. In the calculation with 28 MeV protons, all parameters were chosen identically to the 24 MeV except for the proton energy. As expected the amount of neutrons with higher energy increases with higher proton energy. The increase in the region below 1 MeV is around 30%, while above 10 MeV, it is more than 2 times, both for MCNP6 and FLUKA results. This means that for shielding calculations only a quantitative scaling of the neutron fluence rate at different proton energies without an adjustment of the neutron energy spectrum is not feasible.

Because the neutron spectra are substantially equal in the important energy region for the shielding above 1 MeV, the following shielding calculations were carried out using the results of the MCNP6 calculations (with TENDL data and the point-like source). At an energy of 24 MeV and a current of 300 μA , the neutron source strength is $1.65 \cdot 10^{13}$ n/s, while for 28 MeV protons it is $2.43 \cdot 10^{13}$ n/s.

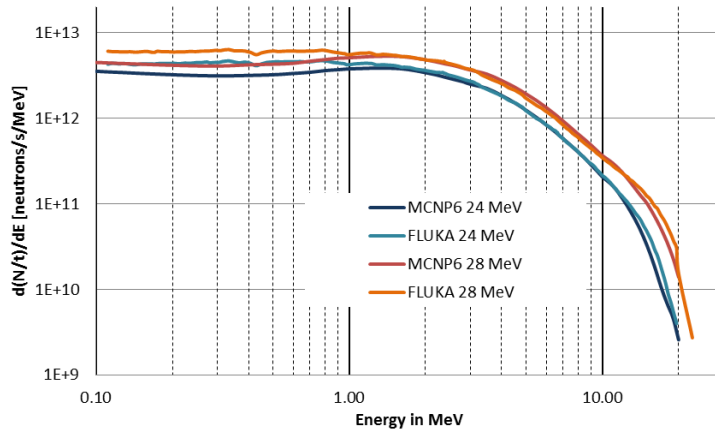


Figure 6: Spectra of neutron rate per MeV of MCNP6 and FLUKA calculations for a point beam with a current of 300 μA . The proton energies were 24 MeV and 28 MeV.

In addition, it was observed that 40% more neutrons were emitted in the forward hemisphere (in direction of point A, see Fig. 1). The radiation source term was modeled as an isotropic point source situated at the target location, the neutron fluence rate was increased by 40% to ensure a realistic description in the proton beam direction and also in the direction towards the points A and B in Fig. 1. Due to this simplification, the calculated dose values are overestimated. However, the additional contribution for the point A and B due to the excess of neutrons emitted in the backward hemisphere will be small because for these neutrons to have an effect on the dose results need to be scattered back from the walls. For the points C and D there is a larger influence. As will be seen in the next section, the results show that the dose rates calculated using this approximation are well below the reference value of 0.5 $\mu\text{Sv/h}$, which means that the simplified source term is appropriate for this purpose.

4. Estimate of the dose rate

As mentioned above, the cyclotron TR-FLEX with nominal proton energy of 28 MeV will be installed at HZDR. We present therefore only results for a 28 MeV proton beam.

According to the described geometrical model (Fig. 2 and 3), the neutron and gamma fluence rates are calculated with the MCNP6 code for a neutron source strength of $2.43 \cdot 10^{13}$ n/s. The dose rates in the points A and B (see Fig. 1) behind the 270 cm thick shielding wall were determined on the basis of particle spectra and the energy-dependent conversion factors. The particle spectra were estimated with a "Point Detector". A point detector is a deterministic estimate of the flux at a point in space [23]. Table 3 shows the resulting total fluence and dose rates. The gamma fluence rates in Table 3 are only for gammas from neutron reactions in the concrete walls. The gamma fluence rates coming from reactions in the water target were calculated separately. The results are shown at the end of this section.

Table 3: Total fluence and dose rates and the corresponding uncertainties at points A, B and D (see Fig. 1) due to the neutrons emitted from the target hit by a 28 MeV proton beam:

particle	point A		point B		point D	
	value	error	value	error	value	error
total fluence rate in particle/s/cm ²						
neutrons	0.057	0.6%	0.020	0.9%	0.027	0.9%
gammas	6.252	0.4%	3.057	0.5%	3.061	0.5%
dose rate in $\mu\text{Sv/h}$						
neutrons	0.004	1.0%	0.001	1.5%	0.002	0.5%
gammas	0.045	0.5%	0.022	0.6%	0.022	0.6%
sum	0.049	0.5%	0.023	0.6%	0.024	0.6%

Table 4: Total fluence and dose rates and the corresponding uncertainties at points A, B and D (see Fig. 1) due to the gammas emitted from the target hit by a 28 MeV proton beam:

Particle	point A		point B		point D	
	value	error	value	error	value	error
total fluence rate in particle/s/cm ²						
gammas	3.325	1.4%	1.375	1.2%	2.077	1.8%
dose rate in $\mu\text{Sv/h}$						
gammas	0.030	1.9%	0.012	1.6%	0.019	1.5%

The calculated total dose rate in point B (at the public road) for neutrons and gammas was estimated to be 0.023 $\mu\text{Sv/h}$. A total value of 0.049 $\mu\text{Sv/h}$ was calculated at point A, a factor of two compared to point B. For point D (vertical direction above the target, just above the 270 cm ceiling) the total dose rate is comparable with the dose rate found in point B.

It can be noted that the calculated fluence and dose rates of the gammas are much larger compared to the ones of the neutrons. This is due to gammas produced by neutron reactions inside the concrete walls.

The partitioning of the shielding wall in zones allows for the possibility to estimate fluence rate values at the zone surfaces. Fig. 7 shows the decrease of the neutron and gamma fluence rates across the wall thickness. The calculated statistical error (1σ) for all values was found to be less than 1%. The curves show a significant smaller decrease of the gamma fluence rate with respect to the neutron fluence rate, resulting in a higher rate after a thickness of about 100 cm. This is due to the fact that the gammas are constantly replenished by neutron reactions.

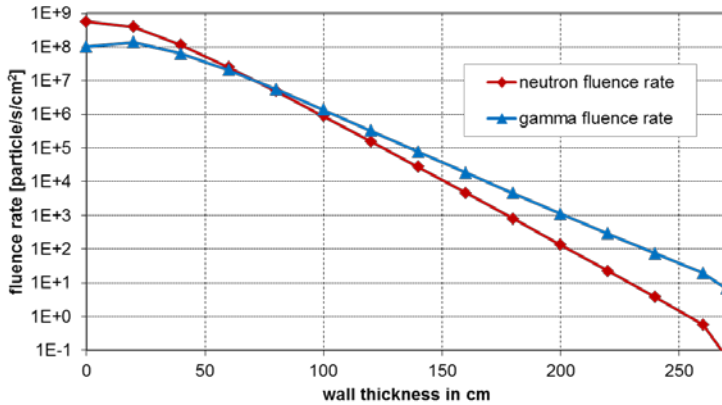


Figure 7: Neutron and gamma fluence rate inside the shielding wall.

Based on these results, the “tenth value thickness” could be determined for the assumed concrete composition by fitting the values in the range between 60 cm and 240 cm. The result is (26.3 ± 0.1) cm for neutrons and (32.8 ± 0.2) cm for gammas.

With MCNP6 the emitted number and spectrum of gammas by the 28 MeV proton beam on water target was also calculated. The emitted gamma source strength was $8.15 \cdot 10^{12}$ gammas/s at a current of 300 μA . Similar calculations like for the neutrons were carried out with the gamma source term. Table 4 shows the results.

A maximum dose rate 0.012 $\mu\text{Sv/h}$ was estimated in point B. This is 50% of the gamma dose rate value in Table 3 from neutron-induced reactions in the walls. The estimated dose rate contribution in point A from the gamma source is 0.03 $\mu\text{Sv/h}$ and in point D 0.019 $\mu\text{Sv/h}$. These estimates show that the gamma source can't be neglected in the estimation of the dose rate.

The total calculated dose rate in the region of the public road is 0.035 $\mu\text{Sv/h}$ (point B), and thus far below the limit of 0.5 $\mu\text{Sv/h}$, corresponding to the effective dose reference figure for the general public (1 mSv per calendar year according to the German Radiation Protection Ordinance). Above the building (point D), the dose rate amounts to 0.043 $\mu\text{Sv/h}$ and will not exceed 0.5 $\mu\text{Sv/h}$.

5. Estimate of the soil activation

In contrast to the walls the ground plate has only a thickness of 60 cm. Consequently, much higher neutron fluence rates occur here outside the concrete. As a result, an undesirably amount of radionuclides could be produced in the

ground during the beam operation. For the estimation of the resulting soil activation for a cyclotron operating with proton energy of 28 MeV and current 300 μA , the average neutron fluence rates in 260 energy groups in a cube with a side length of 20 cm directly below the concrete foundation were calculated with MCNP6 (see Fig. 1, point C). The gamma spectrum was calculated in order to determine possible gamma-induced activation in the soil. The number of gamma energy groups used was 20. At point C (Fig. 1), the total neutron fluence rate was found to be $3.1 \cdot 10^6/\text{s}/\text{cm}^2$, while the total gamma fluence rate was $4.9 \cdot 10^6/\text{s}/\text{cm}^2$, both at a proton beam of 28 MeV and 300 μA . It can be assumed that the real values are approximately 20% smaller due to the assumption of an isotropic source.

The generated radionuclides and the saturation activities in the soil material were determined in a second step with the FLUKA Monte Carlo code, by using the fluence rates for neutrons and gammas mentioned above. The FLUKA geometrical model was a 15 cm x 15 cm x 15 cm cube filled with soil. Particle fluences were conservatively assumed homogeneous and isotropic over the whole volume. The cyclotron operation has been assumed continuous over 5 years with a beam time of 7 hours a day, 5 days a week and 52 weeks a year with the maximum beam parameters. The radiological evaluation of the soil based on individual activity concentrations for this irradiation cycle and corresponding decay times was carried out according to the German Radiation Protection Ordinance [3].

The soil composition which was used in the calculations is listed in Table 5. It is a representable composition which was already used in shielding evaluations for other HZDR facilities [24]. The assumed density of the ground material is 2.0 g/cm^3 .

Table 5: Soil composition in weight percent (wt %) from ref. 24:

	wt %		wt %		wt %
O	53.0	K	1.0	Ni	0.001
Si	32.0	C	1.0	As	0.001
Al	4.0	Mn	0.5	Th	0.0004
Ca	3.0	Cr	0.0055	U	0.0002
Fe	2.0	Zn	0.005	Cd	0.0001
Mg	2.0	Pb	0.005		
Na	1.0	Cu	0.002		

FLUKA calculations of the activities induced by gammas inside the soil volume showed that no production of radionuclides was detected in the considered volume. In principle, this result was expected. The reason is that the potentially possible nuclear reactions have an energy threshold larger than approximately 9 MeV and the share of the spectrum of gammas above this energy is less than 0.5%. The 9 MeV result as a rule-of-thumb value from the binding energy of the nucleons in nuclei [25]. In addition, the reactions usually have a small cross section. For these reasons, the gamma-induced activation of the soil can be neglected. The soil activation is therefore determined only by the neutrons.

An activity concentration of about 78 Bq/g was calculated for the soil directly after the shutdown of the cyclotron after 5 years of operation with a proton beam of 28 MeV and 300 μA . The decay of the total activity is shown in Table 6.

The neutron-induced soil activity is mainly determined by radionuclides with short half-life. Therefore the total activity concentration reduces within 30 days after shutdown of the cyclotron by about two orders of magnitude.

Table 6: Calculated total activity concentration and the corresponding uncertainties (1σ) below the ground plate of the building in dependence of the decay time after shutdown of the cyclotron:

decay time in days	Total activity concentration in Bq/g	error
0	78.34	0.01 %
7	0.47	0.1 %
30	0.34	0.1 %
180	0.10	0.7 %

Fig. 8 shows the total decay activity and the decay activities for the most important nuclides. The change of the nuclide composition over the time changes the value of the unrestricted clearance in accordance with the German Radiation Protection Ordinance. 30 days after shutdown the value for unrestricted clearance of 12.3 Bq/g is obtained (nuclides with a calculated single activity of less 10^{-6} Bq/g were neglected). The total activity concentration 30 days after shutdown is 0.34 Bq/g, this is 2.8 % of the allowed value in ref. 3. The radionuclide

^{37}Ar is the main component of the soil activation until 90 days after shutdown of the facility. The radionuclides ^{45}Ca and ^{55}Fe dominate thereafter.

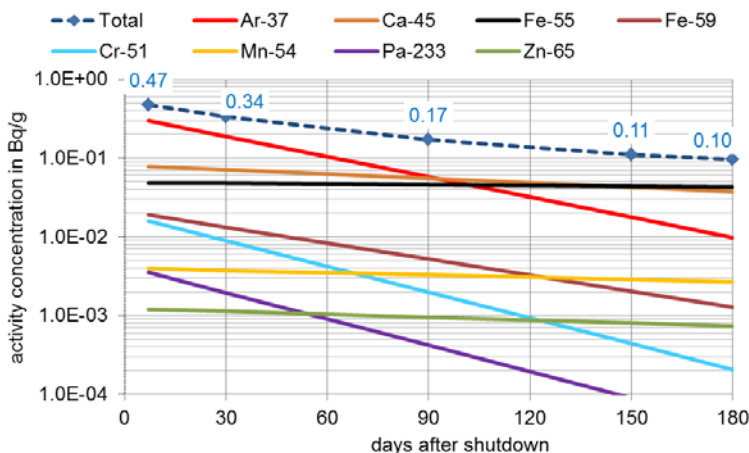


Figure 8: The total decay and the decay of the most important nuclides after 5 years of operation below the ground plate, short-lived radionuclides are not shown.

6. Conclusions

The aim of this document is to demonstrate that the permitted dose rate of $0.5 \mu\text{Sv/h}$ in public places is not exceeded under maximal beam conditions of the new cyclotron to be installed at the HZDR. Based on the neutron and gamma radiation generated by the production of ^{18}F , dose rates were calculated behind a 270 cm thick wall of normal concrete at relevant points outside the cyclotron building. The dose rates were estimated with the Monte Carlo method using the radiation transport code MCNP6. In addition, the soil activation was calculated below the building using the FLUKA code.

The source terms of neutron and gamma emission for the $^{18}\text{O}(p,n)^{18}\text{F}$ reaction were calculated with the MCNP6 code. The emitted particle rate was $2.43 \cdot 10^{13}$ neutrons/s and $8.15 \cdot 10^{12}$ gammas/s with a proton energy of 28 MeV and a current of 300 μA . The results were cross-checked with FLUKA calculations. The calculations show that the maximum dose rates outside the building are far below the legal limit. At a distance of 20 cm from the building wall, at the point B (public road), the neutron source term from the target gives a total dose rate of $0.023 \mu\text{Sv/h}$. The dose rate of gammas originating from the ^{18}O target amounts to $0.012 \mu\text{Sv/h}$. The calculations show that these gammas from nuclear reactions in the target can contribute in a non-negligible way to the total dose rate. The total dose rate outside the building amounts to $0.035 \mu\text{Sv/h}$.

The generated radionuclides and the saturation activities in soil material under the ground plate were determined with the particle transport program FLUKA on the basis of the neutron fluence rate calculated with MCNP6. To determine the activities it is assumed that the cyclotron is operated over 5 years (see section 5). It was shown that the activities are mainly created by radionuclides with short half-life time. For maximum proton energy of 28 MeV and a current of 300 μA a total activity concentration of about 78 Bq/g was calculated for the soil right after shutdown of the cyclotron. After a decay time of 30 days a value of 0.34 Bq/g was calculated. Under these conditions after 30 days the value of 12.3 Bq/g is permitted for the unrestricted clearance in accordance with the German Radiation Protection Ordinance⁴. Thus, 2.8 % of the maximally allowed value is exhausted.

For energy of 24 MeV a neutron source term was provided by the manufacturer. This source term is obtained only on the basis of the yield calculated for $^{18}\text{O}(p,n)^{18}\text{F}$ reaction and using differential cross sections calculated with ALICE-91. In this case the maximum emitted neutron rate was $1.65 \cdot 10^{13}$ n/s for a proton beam current of 300 μA . The comparison of calculated emitted neutron rates showed that the rates obtain with MCNP6 and FLUKA were about 5 times larger than the one provided by the manufacturer. The reason is that a calculation based on the ^{18}F activity only doesn't include all neutron-producing reactions, and can lead to an underestimation of the actual shielding requirements. Given the importance of our results, we have started an experimental program to validate our simulation results, since the basis of all shielding calculations is a reliable calculation of the radiation source term.

Acknowledgment

We thank the project manager Mr. Preusche of HZDR for his assistance and support.

References

1. Goorley, T. et al. *Initial MCNP6 Release Overview*, Nuclear Technology **180**, pp 298 - 315 (2012).
2. Ferrari, A., Sala P.R., Fasso, A. and Ranft, J. *FLUKA: a multi-particle transport code*, CERN-2005-10, INFN/TC_05/11, SLAC-R-773 (2005).
3. *Strahlenschutzverordnung*, 9. Auflage vom 01.11.2011, Bundesanzeiger Verlag (2011).
4. Facure, A. and Franca, W.F. *Optimal shielding design for bunkers of compact cyclotrons used in the production of medical radionuclides*, Med Phys **37** 6332-7 (2010).
5. Bosko, A., Zhilchenkov, D., and Reece, W.D. *GE PETtrace cyclotron as a neutron source for boron neutron capture therapy*, Appl. Radiat. Isot. **61** 1057–62 (2004).
6. Pevey, R., Miller, F.L., Marchall, B.J., Townsend, L.W. and Alord, B. *Shielding for a Cyclotron used for Medical Isotope Production in China*, Radiation Protection Dosimetry, vol. 115 415-419 (2005).
7. Dalle, H.M. and Campolina, D. *Shielding Simulation of the CDTN Cyclotron Bunker Using MCNP*, International Nuclear Atlantic Conference –INAC 2011 Belo Horizonte, MG, Brazil, Oct. 24-28 (2011).
8. Sheu, R.J., Sheu, R.D., Jiang S.H., Kao, C.H. *Adjoint Acceleration of Monte Carlo Simulations Using TORT/MCNP Coupling Approach: a Case Study on the Shielding Improvement for the Cyclotron Room of the Buddhist TZU CHI General Hospital*, Radiation Protection Dosimetry, vol. 113 140-151 (2005).
9. Som, P., et al. *A fluorinated glucose analog, 2-fluoro-2-deoxy-D-glucose (F-18): Nontoxic tracer for rapid tumor detection*, J. Nucl. Med. **21** (7), p. 670–675 (1980).
10. *Conversion Coefficients for use in Radiological Protection against External Radiation*, International Commission on Radiation Units & Measurements, 7910 Woodmont Avenue Bethesda, Maryland 20814, USA, ICRU Report **57** (1998)
11. *ICRP, Conversion Coefficients for use in Radiological Protection against External Radiation*, ICRP Publication **74**. Ann. ICRP 26 (3-4) (1996).
12. Newman, J. and Choo, B.S. *Advanced Concrete Technology*, Butterworth Heinemann, ISBN 0 7506 5105 9 (2003).
13. Chadwick M.B., et al. *ENDF/B-VII.1 Nuclear Data for Science and Technology: Cross Sections, Covariances, Fission Product Yields and Decay Data*, Nuclear Data Sheets, Volume 112, Issue 12, p. 2887-3152 (2011).
14. *Final Report – Monte Carlo Simulation of TR 24 Shielding (Sherbrooke Project)*, documentation supplied with TR-FLEX cyclotron, Advanced Cyclotron Systems, Inc., Richmond, Canada (2011).
15. Blann, M. *ALICE-91, Statistical Model Code System with Fission Competition*, RSIC Code, PACKAGE PSR-146 (1991).
16. Weisskopf, V.F. and Ewing, D.H. *On the Yield of Nuclear Reactions with Heavy Elements*, Phys. Rev. **57**, 472 (1940)
17. Koning, A.J. and Rochman, D. *Modern nuclear data evaluation with the TALYS code system*, Nucl. Data Sheets **113**, 2841 (2012).
18. MacFarlane, R. and Kahler, A. *Methods for Processing ENDF/B-VII with NJOY*, Nuclear Data Sheets **111**, pp. 2739-2890, (2010).
19. Ferrari A., Sala P.R., *A new model for hadronic interactions at intermediate energies for the FLUKA code*, Proc. MC93 Int. Conf. on Monte Carlo Simulation in High Energy and Nuclear Physics, p.277-288, Tallahassee (Florida), 22-26 Feb. 1993. Ed. by P. Dragovitsch, S.L. Linn, M. Burbank, World Scientific, Singapore (1994).
20. CSEWG-Collaboration *Evaluated Nuclear Data File ENDF/B-VI.8*, released in October 2001, (Available from <http://www.nndc.bnl.gov/endl>) (2001).
21. Carroll L.R. *Estimating the Radiation Source Term for PET Isotope Targets*, Poster Presentation at the 9th International Workshop on Targetry and Target Chemistry, Turku, Finland; May 23 - 25 (2002).
22. *Charged particle cross-section database for medical radioisotope production: diagnostic radioisotopes and monitor reactions*, IAEA, Vienna, IAEA-TECDOC-1211, ISSN 1011-4289 (2001).
23. Lux I., Koblinger L., *Monte Carlo Particle Transport Methods: Neutron and Photon calculations*, CRC Press Inc., Boca Raton, Florida (USA), ISBN 0-8493-6074-9 (1991).
24. Rogov, A. *Rechnungen zur Bodenaktivierung bei Betrieb des 6-MV-Tandetrans*, Anlage A.5.3 im 1. Sicherheitsbericht (2009).
25. Evans, R. D.: *The Atomic Nucleus*, McGraw Hill, New York 1955